Georgia Tech College of Computing
School of Computational
Science and Engineering

2025 MFEM Community Workshop

Structure-Preserving Transfer of Grad-Shafranov Equilibria to Magnetohydrodynamic Solvers

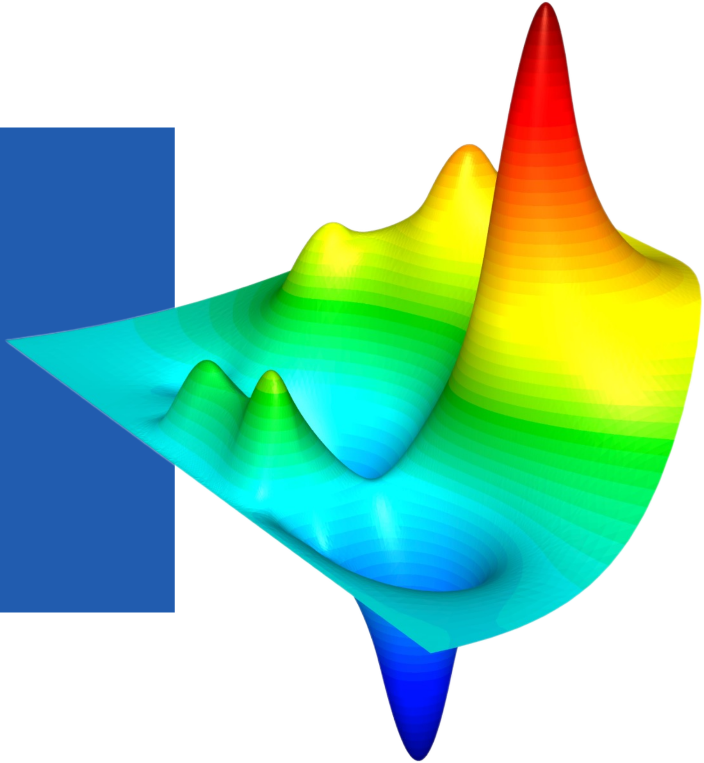

Rushan Zhang, Golo Wimmer and Qi Tang

Ph.D. Student, Computational Science and Engineering
Georgia Institute of Technology

MFEM Grad-Shafranov (GS) solver for axisymmetric equilibrium (2024 MFEM workshop)

Assuming axisymmetry in a tokamak, we can represent $\mathbf{B}$ with poloidal flux function $\mathbf{\Psi}$ and toroidal field function f,

Force Balancing $\mathbf{J} \times \mathbf{B} = \nabla p,$

MHD Approx. $\mu \mathbf{J} = \nabla \times \mathbf{B},$ $\Longrightarrow \Delta^* \Psi := r\partial_r \left(\frac{1}{r} \partial_r \Psi \right) + \partial_z^2 \Psi = -\mu r^2 p'(\Psi) - f(\Psi) f'(\Psi)$

Tokamak Rep. $\mathbf{B} = \nabla \times \left(\frac{\Psi}{r} \mathbf{e}_\phi \right) + \frac{f}{r} \mathbf{e}_\phi.$

Therefore, the governing equations become,

$$-\frac{1}{\mu r} \Delta^* \Psi = \begin{cases} r p'(\Psi) + \frac{1}{\mu r} f(\Psi) f'(\Psi), & \text{in } \Omega_p(\Psi), \\ I_i / |\Omega_{c_i}|, & \text{in } \Omega_{c_i}, \\ 0, & \text{elsewhere in } \Omega_\infty \end{cases}$$

$$\Psi(0, z) = 0,$$

$$\lim_{\|(r,z)\| \to +\infty} \Psi(r, z) = 0$$

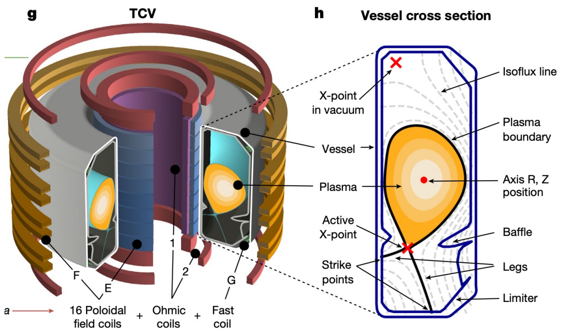

D. Serino, Q. Tang, X.-Z. Tang, T. V. Kolev, and K. Lipnikov.
An adaptive Newton-based free-boundary Grad–Shafranov solver, SISC, 2025

DeepMind and EPFL, Nature, 2022

Task: transfer of GS equilibria to MHD solvers

GS equation solves for $\boldsymbol{\Psi}$ and f while MHD simulations need the $\mathbf{B}$ field directly.

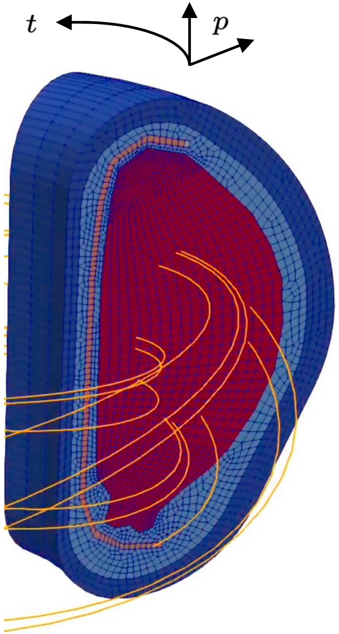

Consider

$$\mu \mathbf{J} = \nabla \times \mathbf{B},$$

$$\mathbf{B} = \underbrace{\nabla \times \left(\frac{\Psi}{r} \mathbf{e}_\phi \right)}_{\mathbf{B}_p} + \underbrace{\frac{f}{r} \mathbf{e}_\phi}_{B_t}.$$

Thus we have the $\mathbf{B}$ fields

$$\mathbf{B}_p = \frac{1}{r} \nabla^\perp \Psi, \qquad B_t = \frac{f}{r},$$

and the $\mathbf{J}$ fields

$$\mu \mathbf{J}_p = \frac{1}{r} \nabla^\perp (r B_t), \qquad \mu J_t = -\nabla^\perp \cdot \mathbf{B}_p.$$

Goal: investigate errors during the transfer process

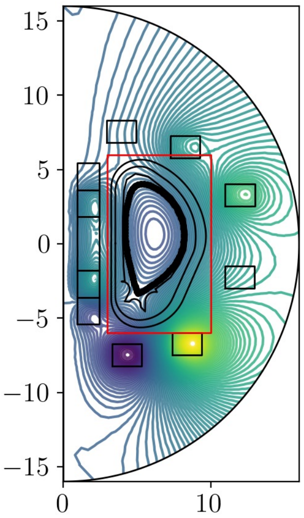

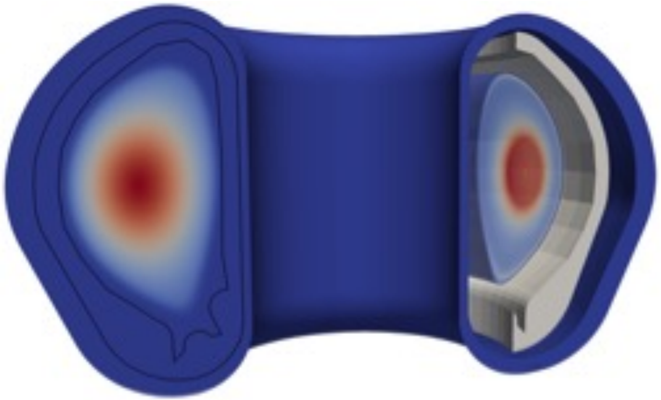

The transfer process is prone to numerical errors:

- **Source 1:** incompatibilities between the GS and MHD FEM spaces,
- **Source 2:** difference between the GS and MHD meshes,
- **Source 3:** discontinuities at the separatrix.

Unnatural projection is unavoidable in compatible FEM

In compatible FEM, we have the natural **FEM spaces** that corresponds to **differential operators**,

$$CG \xrightarrow{\nabla} H(\text{curl}) \xrightarrow{\nabla^{\perp}\cdot} DG, \qquad CG \xrightarrow{\nabla^{\perp}} H(\text{div}) \xrightarrow{\nabla\cdot} DG\ .$$

Consider **Ψ and f both in CG field**, the most natural projection path is,

$$\Psi \in CG(\mathcal{T}_{2D})_m \quad \to \quad \mathbf{B}_p \in H(\text{div}, \mathcal{T}_{2D})_m \quad \to \quad J_t \in CG(\mathcal{T}_{2D})_m,$$

$$f \in CG(\mathcal{T}_{2D})_m \quad \to \quad B_t \in CG(\mathcal{T}_{2D})_m \quad \to \quad \mathbf{J}_p \in H(\text{div}, \mathcal{T}_{2D})_m.$$

However, **$H(\text{div})$** for poloidal direction corresponds to **DG** for toroidal direction in stead of **CG**.

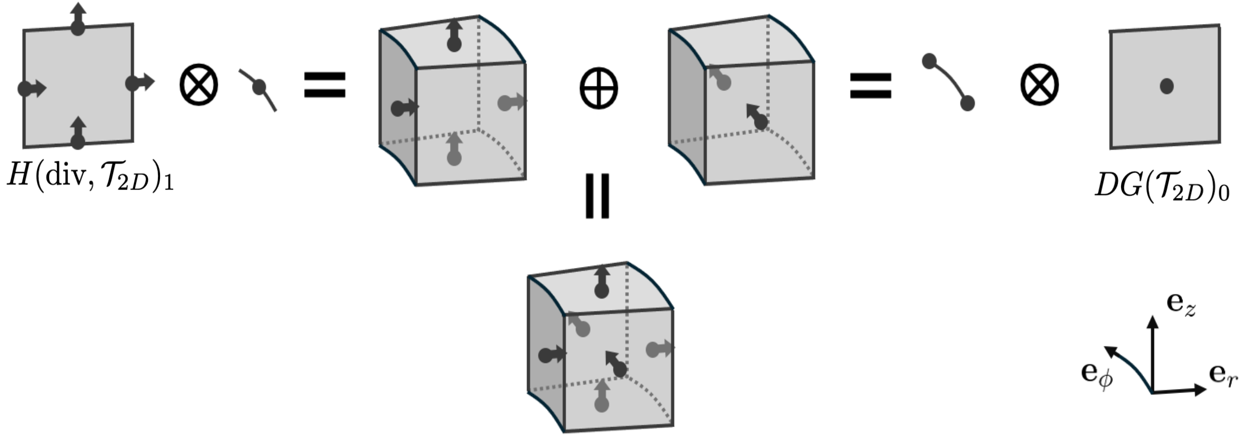

Source 1: incompatibilities between the GS and MHD FEM spaces

Thus, we have the following **three projection paths** to experiment:

Compatible Finite Element

$$\Psi \in CG(\mathcal{T}_{2D})_m \rightarrow \mathbf{B}_p \in H(\mathrm{div}, \mathcal{T}_{2D})_m \rightarrow J_t \in CG(\mathcal{T}_{2D})_m,$$
$$f \in CG(\mathcal{T}_{2D})_m \rightarrow B_t \in DG(\mathcal{T}_{2D})_{m-1} \rightarrow \mathbf{J}_p \in H(\mathrm{curl}, \mathcal{T}_{2D})_m. \quad (1)$$

$$\Psi \in CG(\mathcal{T}_{2D})_m \rightarrow \mathbf{B}_p \in H(\mathrm{curl}, \mathcal{T}_{2D})_m \rightarrow J_t \in DG(\mathcal{T}_{2D})_{m-1},$$
$$f \in CG(\mathcal{T}_{2D})_m \rightarrow B_t \in CG(\mathcal{T}_{2D})_m \rightarrow \mathbf{J}_p \in H(\mathrm{div}, \mathcal{T}_{2D})_m. \quad (2)$$

Red box: unnatural projection steps

Vector CG

$$\Psi \in CG(\mathcal{T}_{2D})_m \rightarrow \mathbf{B}_p \in CG(\mathcal{T}_{2D})_m^2 \rightarrow J_t \in CG(\mathcal{T}_{2D})_m,$$
$$f \in CG(\mathcal{T}_{2D})_m \rightarrow B_t \in CG(\mathcal{T}_{2D})_m \rightarrow \mathbf{J}_p \in CG(\mathcal{T}_{2D})_m^2. \quad (3)$$

Source 2: difference between the GS and MHD meshes

To examine the impact from mesh misalignment, we apply **a very small perturbation ($\alpha = 0.05$)** to the original mesh:

$$r_i' = r_i + \alpha \sin(r_i), \qquad z_i' = z_i + \alpha \sin(z_i).$$

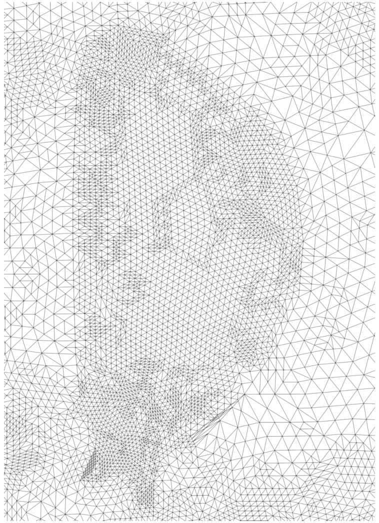

Original

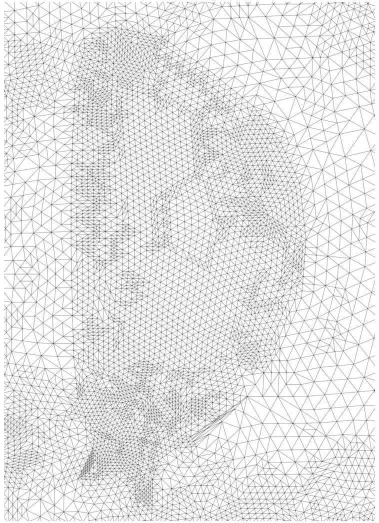

Perturbed

Source 3: discontinuities at the separatrix.

To examine the impact from the discontinuities at the separatrix, we conduct experiments with **mesh refinement** and **alignment** along the separatrix:

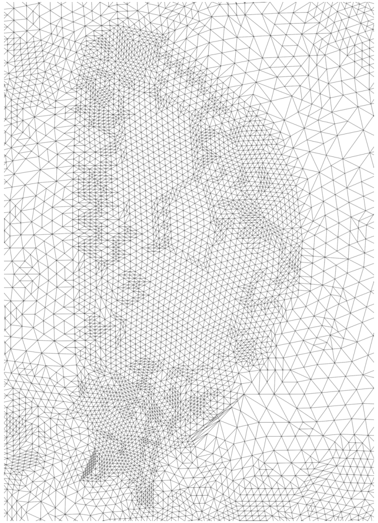
Original

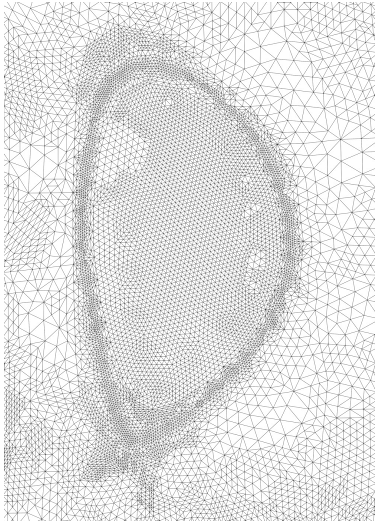
Refined

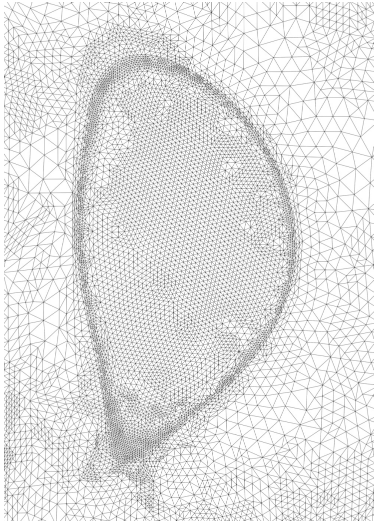
Refined + aligned

Equilibrium solution for experiments – Taylor state equilibrium

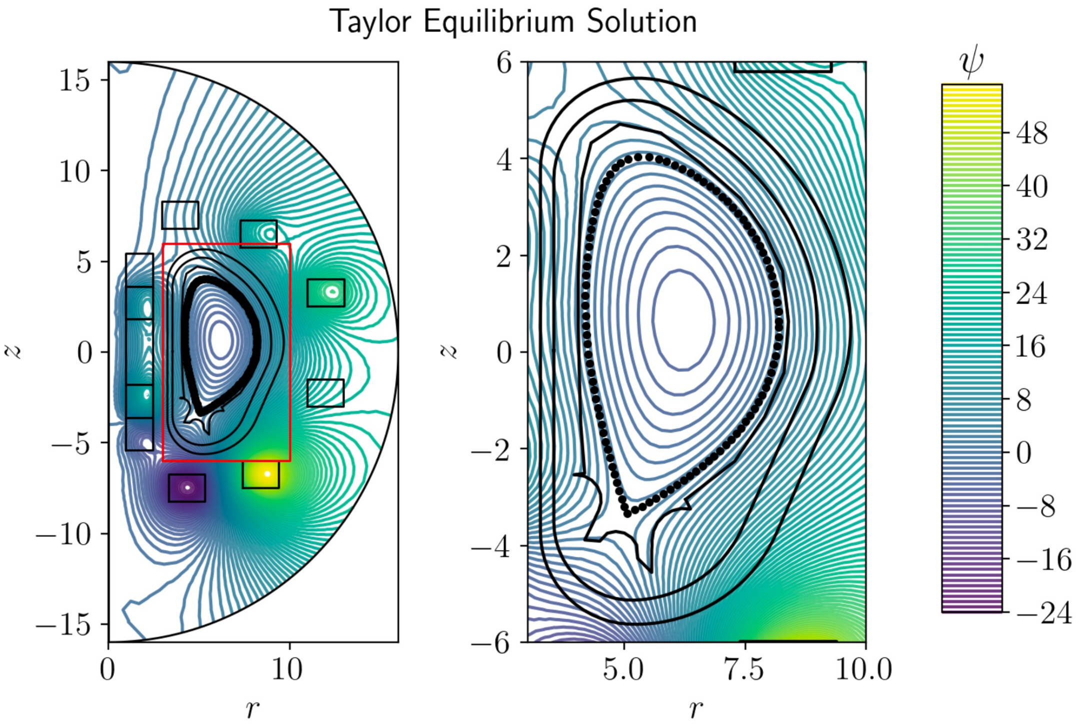

Numerical solution and its zoom-in

D. Serino, Q. Tang, X.-Z. Tang, T. V. Kolev, and K. Lipnikov. An adaptive Newton-based free-boundary Grad–Shafranov solver, SISC, 2025

Force balancing – projection paths

$$\begin{aligned} \Psi \in CG(\mathcal{T}_{2D})_m &\rightarrow \mathbf{B}_p \in H(\mathrm{div}, \mathcal{T}_{2D})_m \rightarrow J_t \in CG(\mathcal{T}_{2D})_m, \\ f \in CG(\mathcal{T}_{2D})_m &\rightarrow B_t \in DG(\mathcal{T}_{2D})_{m-1} \rightarrow \mathbf{J}_p \in H(\mathrm{curl}, \mathcal{T}_{2D})_m. \end{aligned} \tag{1}$$

$$\begin{aligned} \Psi \in CG(\mathcal{T}_{2D})_m &\rightarrow \mathbf{B}_p \in H(\mathrm{curl}, \mathcal{T}_{2D})_m \rightarrow J_t \in DG(\mathcal{T}_{2D})_{m-1}, \\ f \in CG(\mathcal{T}_{2D})_m &\rightarrow B_t \in CG(\mathcal{T}_{2D})_m \rightarrow \mathbf{J}_p \in H(\mathrm{div}, \mathcal{T}_{2D})_m. \end{aligned} \tag{2}$$

$$\begin{aligned} \Psi \in CG(\mathcal{T}_{2D})_m &\rightarrow \mathbf{B}_p \in CG(\mathcal{T}_{2D})_m^2 \rightarrow J_t \in CG(\mathcal{T}_{2D})_m, \\ f \in CG(\mathcal{T}_{2D})_m &\rightarrow B_t \in CG(\mathcal{T}_{2D})_m \rightarrow \mathbf{J}_p \in CG(\mathcal{T}_{2D})_m^2. \end{aligned} \tag{3}$$

$\mu[\mathbf{B} \times \mathbf{J}]_p \in H(\mathrm{div}, \mathcal{T}_{2D})_m$ (1) $\quad \mu[\mathbf{B} \times \mathbf{J}]_p \in H(\mathrm{curl}, \mathcal{T}_{2D})_m$ (2) $\quad \mu[\mathbf{B} \times \mathbf{J}]_p \in CG(\mathcal{T}_{2D})_m^2$ (3)

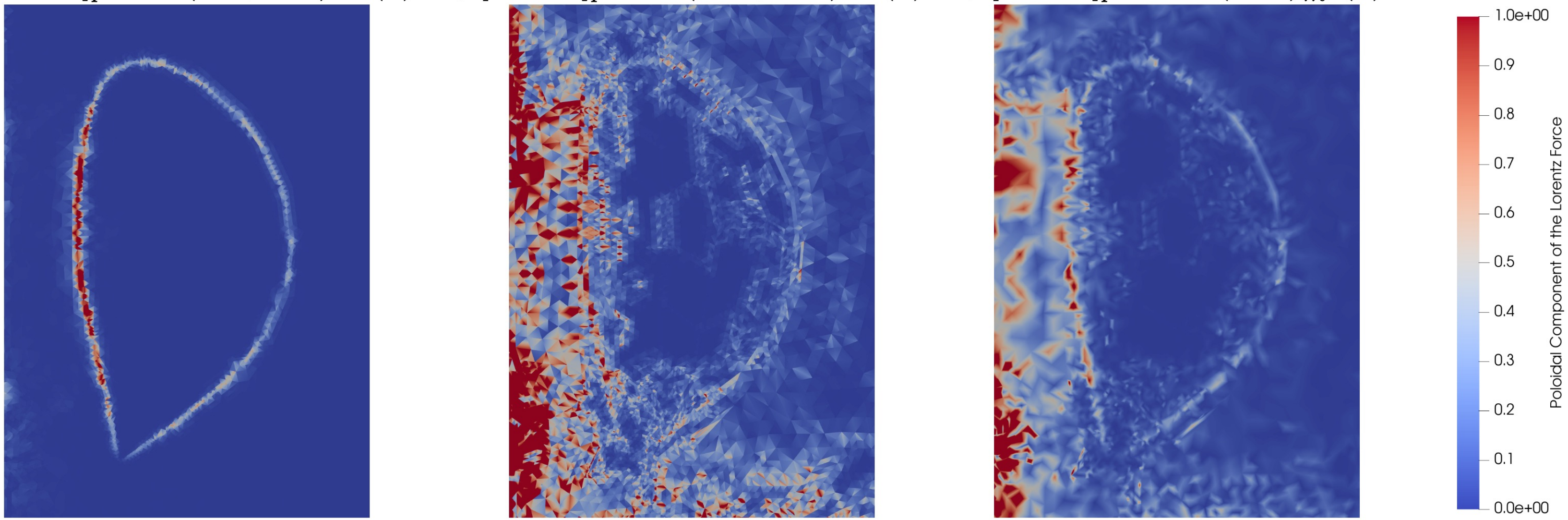

Divergence error – projection paths

$$\Psi \in CG(\mathcal{T}_{2D})_m \rightarrow \mathbf{B}_p \in H(\text{div}, \mathcal{T}_{2D})_m \rightarrow J_t \in CG(\mathcal{T}_{2D})_m,$$
$$f \in CG(\mathcal{T}_{2D})_m \rightarrow B_t \in DG(\mathcal{T}_{2D})_{m-1} \rightarrow \mathbf{J}_p \in H(\text{curl}, \mathcal{T}_{2D})_m. \quad (1)$$

$$\Psi \in CG(\mathcal{T}_{2D})_m \rightarrow \mathbf{B}_p \in H(\text{curl}, \mathcal{T}_{2D})_m \rightarrow J_t \in DG(\mathcal{T}_{2D})_{m-1},$$
$$f \in CG(\mathcal{T}_{2D})_m \rightarrow B_t \in CG(\mathcal{T}_{2D})_m \rightarrow \mathbf{J}_p \in H(\text{div}, \mathcal{T}_{2D})_m. \quad (2)$$

$$\Psi \in CG(\mathcal{T}_{2D})_m \rightarrow \mathbf{B}_p \in CG(\mathcal{T}_{2D})_m^2 \rightarrow J_t \in CG(\mathcal{T}_{2D})_m,$$
$$f \in CG(\mathcal{T}_{2D})_m \rightarrow B_t \in CG(\mathcal{T}_{2D})_m \rightarrow \mathbf{J}_p \in CG(\mathcal{T}_{2D})_m^2. \quad (3)$$

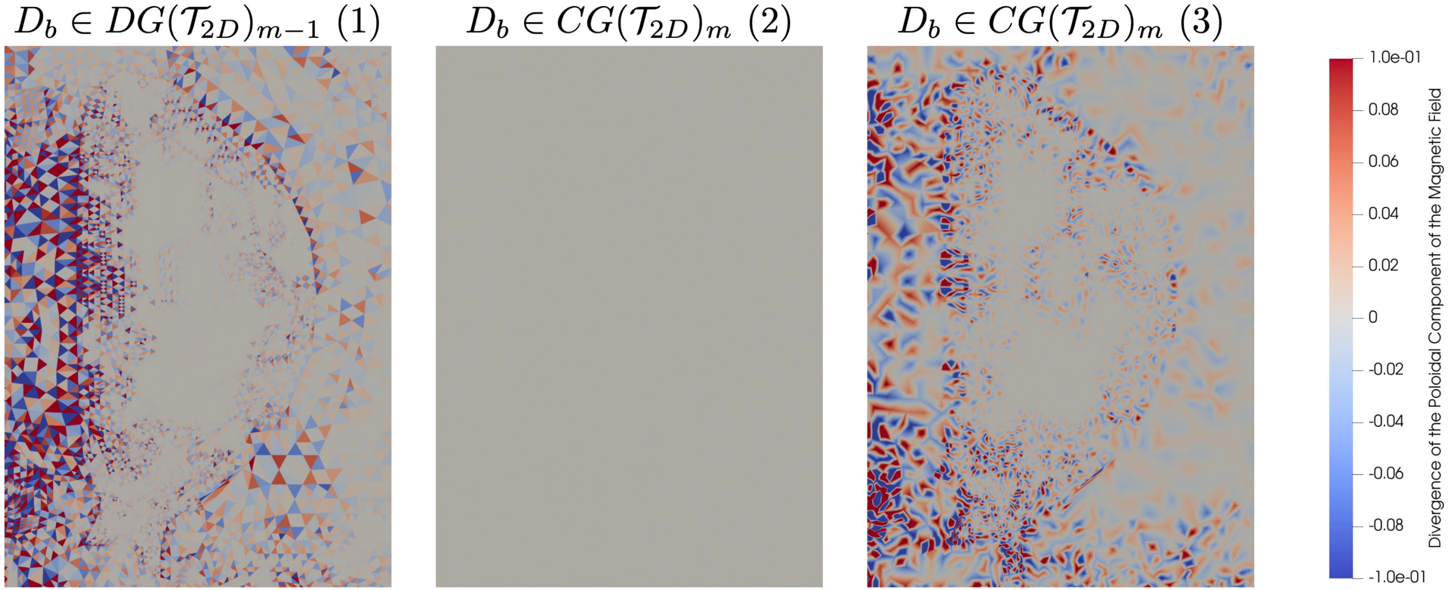

Force balancing – mesh misalignment

$$r_i' = r_i + \alpha \sin(r_i), \qquad z_i' = z_i + \alpha \sin(z_i).$$

$$\alpha = 0.05.$$

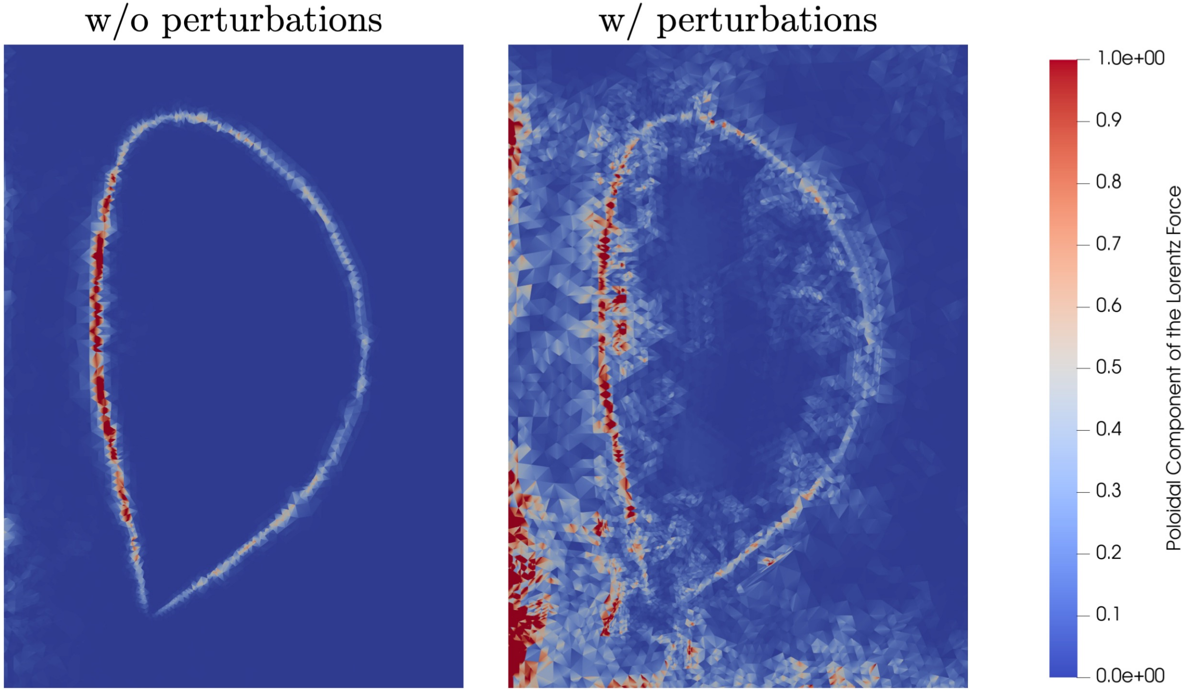

Force balancing - discontinuities at the separatrix

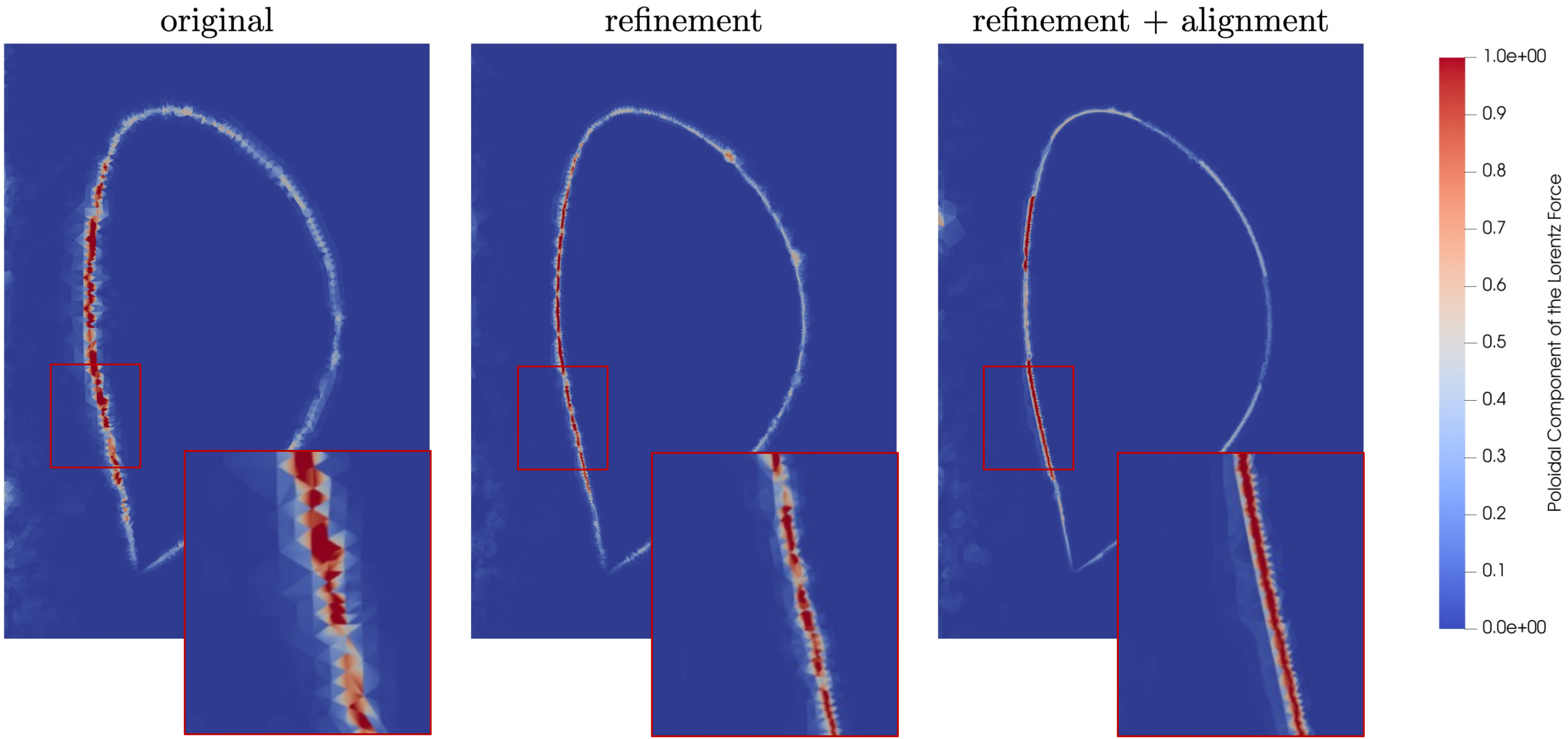

Conclusions

$$\begin{aligned}
\Psi \in CG(\mathcal{T}_{2D})_m &\rightarrow \mathbf{B}_p \in H(\mathrm{div}, \mathcal{T}_{2D})_m \rightarrow J_t \in CG(\mathcal{T}_{2D})_m, \\
f \in CG(\mathcal{T}_{2D})_m &\rightarrow B_t \in DG(\mathcal{T}_{2D})_{m-1} \rightarrow \mathbf{J}_p \in H(\mathrm{curl}, \mathcal{T}_{2D})_m.
\end{aligned} \tag{1}$$

$$\begin{aligned}
\Psi \in CG(\mathcal{T}_{2D})_m &\rightarrow \mathbf{B}_p \in H(\mathrm{curl}, \mathcal{T}_{2D})_m \rightarrow J_t \in DG(\mathcal{T}_{2D})_{m-1}, \\
f \in CG(\mathcal{T}_{2D})_m &\rightarrow B_t \in CG(\mathcal{T}_{2D})_m \rightarrow \mathbf{J}_p \in H(\mathrm{div}, \mathcal{T}_{2D})_m.
\end{aligned} \tag{2}$$

$$\begin{aligned}
\Psi \in CG(\mathcal{T}_{2D})_m &\rightarrow \mathbf{B}_p \in CG(\mathcal{T}_{2D})_m^2 \rightarrow J_t \in CG(\mathcal{T}_{2D})_m, \\
f \in CG(\mathcal{T}_{2D})_m &\rightarrow B_t \in CG(\mathcal{T}_{2D})_m \rightarrow \mathbf{J}_p \in CG(\mathcal{T}_{2D})_m^2.
\end{aligned} \tag{3}$$

- The **choice of finite element spaces** and **mesh alignment** matter.
- Project path (1) is preferred for **force balancing**, whereas path (2) is preferred for **divergence-free**.
- **Mesh refinement** near the separatrix is important, whereas alignment with separatrix is less so.

Future work

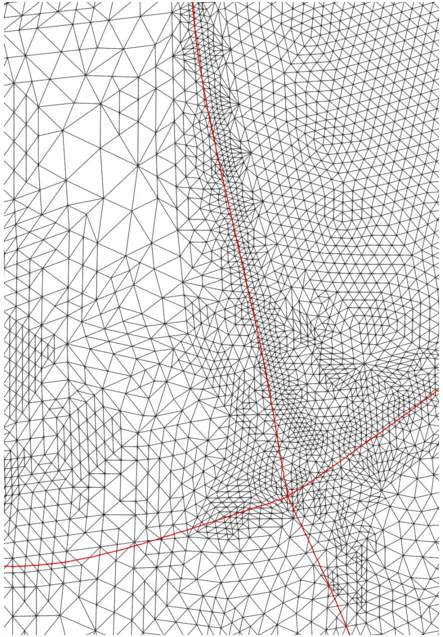

Refined

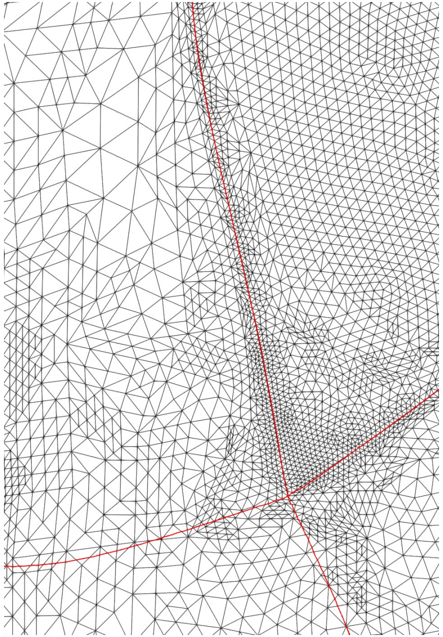

Refined + aligned

Explore TMOP to automatically align the mesh with separatrix during the GS solver, which can be important for transient MHD simulations such as its anisotropic diffusion.

Thank you!

Q&A

Appendix

Component-wise projection of 3D fields

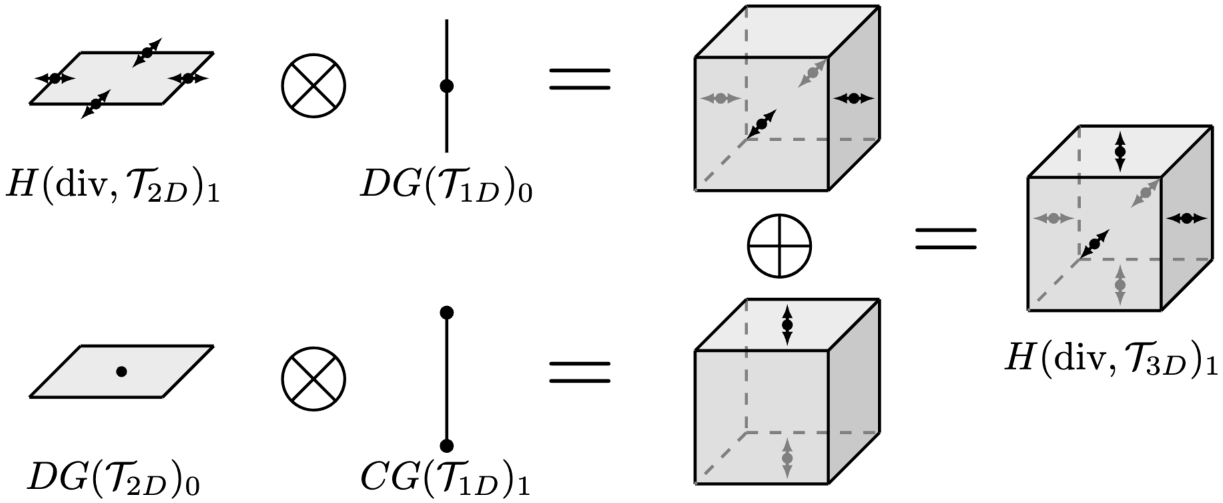

Appendix

3D periodic table of finite-element spaces

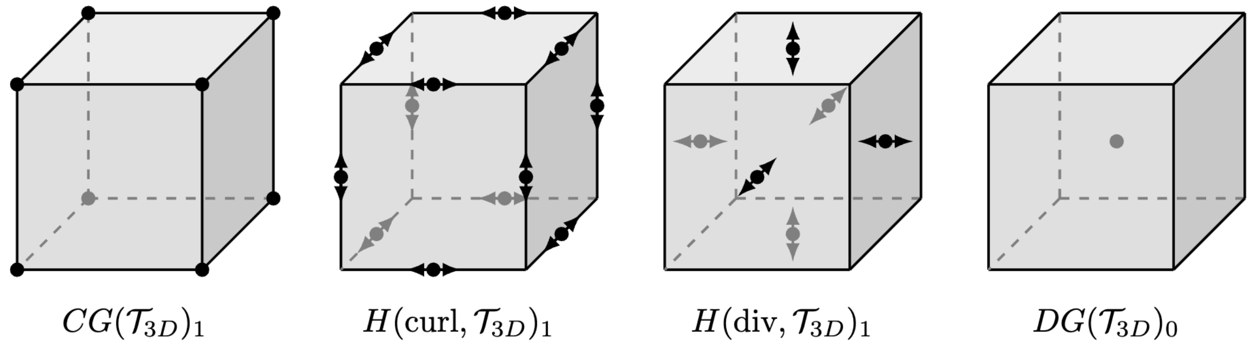

Appendix

Mesh with refinement and mesh with both refinement and alignment

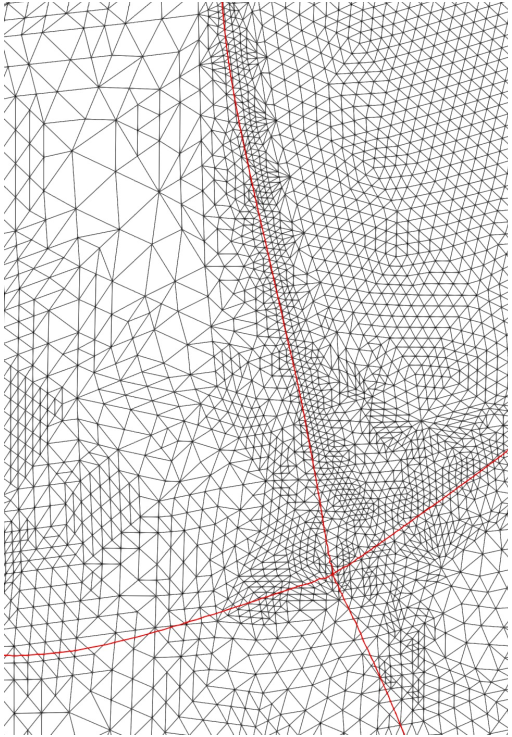

Refined

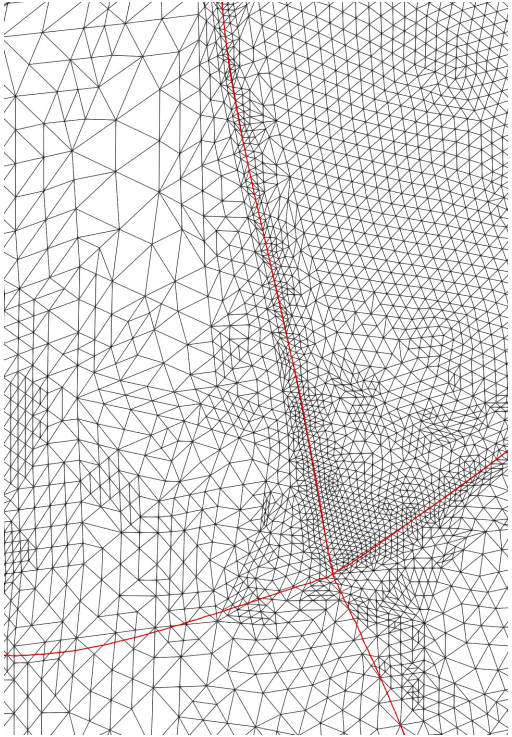

Refined + aligned